

Contrat GIP MERCATOR - CNRS n° 2004/10005
Développement de SAM-2

Rapport final

Période concernée: du 15-03-04 au 15-02-05

Personnel impliqué au LEGI:

Nom	Fonction	Responsabilité	Affectation
J.M. Brankart	IR CNRS	Responsable scientifique	30 %
P. Brasseur	CR CNRS	Assimilation de données	10 %
Y. Ourmières	CDD Mercator	Développements et expérimentations numériques	100 %
L. Berline	Thésard BDI CNRS/CNES	Assimilation pour le couplage physico-biogéochimique	20 %

Rappel introductif

Ce travail s'inscrit dans le cadre de l'accompagnement scientifique au développement du schéma SAM-2, au sein de la collaboration MERCATOR OCEAN – LEGI. Les travaux réalisés pour cette étude ont débuté en mars 2004, avec le recrutement de Yann Ourmières sur un contrat ingénieur réseau bleu MERCATOR d'une durée de 11 mois.

Le système d'assimilation MERCATOR SAM-2 repose sur le concept de correction séquentielle de la trajectoire océanique simulée par un modèle. Cette correction est réalisée de manière intermittente en utilisant les observations disponibles pendant le dernier cycle d'assimilation. De plus, la relative pauvreté de la couverture observationnelle en océanographie rend nécessaire l'utilisation de cycles d'assimilation assez longs (typiquement une semaine) afin que l'analyse statistique se base sur un nombre de données suffisant et ne pâtit pas trop d'inévitables approximations sur la paramétrisation de la covariance des erreurs. La conséquence de cette situation (peu d'observations et cycles d'assimilation longs) est que la correction appliquée au modèle à chaque cycle peut souvent ne pas être petite par rapport au signal qui doit être contrôlé.

Ceci conduit à deux types de problèmes: (i) des discontinuités spatiales et temporelles significatives dans la solution obtenue, et (ii) un état initial qui n'est pas forcément en équilibre dynamique, générant des oscillations parasites à haute fréquence et pouvant conduire à un rejet des données venant d'être assimilées. Ces deux problèmes tendent à limiter sérieusement la capacité prévisionnelle du système opérationnel.

Ce projet vise précisément à l'élimination de ces deux problèmes du système d'assimilation, par l'implémentation d'une technique nouvelle, répandue dans les systèmes d'assimilation séquentielle pour modèles atmosphériques mais relativement récente et peu usitée pour les modèles de prévision océanique. Cette technique appelée Incremental Analysis Update (IAU) pourrait présenter plusieurs avantages pour la configuration actuelle. Tout d'abord, l'utilisation de l'IAU permet d'obtenir

une solution du modèle continue dans le temps. De plus, l'IAU s'avère efficace pour la minimisation d'ondes parasites à haute fréquence, induites par l'étape d'analyse ainsi que pour l'obtention d'états du modèle plus stables que ceux obtenus par une méthode d'assimilation séquentielle classique. Enfin, cette méthode pourrait aussi permettre de corriger le biais modèle de façon continue.

Les principaux objectifs techniques de ce travail sont l'implémentation de cette technique d'IAU et l'étude de son impact sur la solution obtenue. La méthode d'assimilation utilisée pour ces tests est le filtre SEEK. Il s'agit d'un filtre de Kalman de rang réduit développé depuis plusieurs années au LEGI, et qui a servi de précurseur au système d'assimilation SAM2 de MERCATOR. Il a été notamment appliqué à l'assimilation de données d'altimétrie et de température de surface dans un modèle de l'Atlantique Nord au 1/3° (MNATL). Et c'est ce travail (thèse et postdoctorat de Charles-Emmanuel Testut au LEGI) qui a servi de banc d'essai préalable au transfert de cette technologie vers le projet MERCATOR. Donc, bien qu'utilisant ce précurseur de SAM2 (basé sur le logiciel SESAM) et non SAM2, le banc d'essai utilisé pour cette nouvelle étude (l'évaluation de l'IAU) est donc parfaitement compatible avec le système d'assimilation actuel de MERCATOR.

Les quelques différences entre ce système et SAM2, notamment l'utilisation d'un vecteur d'estimation sensiblement différent (U,V,T,S au lieu de ψ, T, S) ou l'utilisation d'un modèle à toit rigide, n'affectent en rien l'utilité pour MERCATOR des résultats obtenus car, d'une part, les corrections incrémentales appliquées ne se portent que sur les champs de température et de salinité, et, d'autre part, des tests en configuration à surface libre ont montré que la technique IAU pouvait être facilement adaptée à ce genre de configuration. Par ailleurs, comme le développement d'une technique telle que l'IAU se fait relativement indépendamment du schéma d'analyse utilisé, elle peut être virtuellement implantée telle quelle dans n'importe quel système d'assimilation séquentielle et donc, sans aucun doute, dans le système SAM2 de MERCATOR.

Par conséquent, les résultats présentés dans le rapport joint sont fortement axés sur la démonstration de l'impact général de l'implémentation de la technique IAU dans le système d'assimilation SEEK employé. Et toutes les conclusions qui y sont tirées sont bien sûr intégralement transposables à SAM2.

Veillez trouver ci-joint le rapport complet d'activité en langue anglaise.

Table of contents

Abstract	4
1) Introduction	4
<i>a. Atmospheric General Circulation Models (AGCM)</i>	5
<i>b. Ocean General Circulation Models (OGCM)</i>	6
<i>c. Discussion</i>	8
2) Model configuration and IAU implementation	8
<i>a. Model configuration</i>	8
<i>b. Data assimilation scheme</i>	9
<i>c. IAU methodology</i>	9
3) The conducted experiments	11
4) Results	12
<i>a. High frequency oscillations</i>	13
1) <i>Oscillation filtering</i>	13
2) <i>Signal filtering and modification</i>	15
3) <i>Spurious trajectories at isolated grid points</i>	16
4) <i>Oscillations duration</i>	18
<i>b. Time continuity</i>	20
<i>c. RMS difference with the assimilated data</i>	21
<i>d. Spatial averaged field evolution</i>	22
<i>e. Global EKE production</i>	24
<i>f. Gulf stream structure modification</i>	25
<i>g. Comparisons with independent data: moorings</i>	28
5) Conclusion and perspectives	30
References	31
Technical Appendix	33
A. IAU implementation	33
1. Model modifications	33
2. Assimilation system modifications	36
B. High frequency outputs	36

Incremental Analysis Update implementation into the intermittent data assimilation system using the SEEK filter for the ocean general circulation model OPA 8.1 in the North Atlantic 1/3° configuration NATL3.

Y. Ourmieres*, J.M. Brankart*, L. Berline* and P. Brasseur*.

*LEGI, BP53X, 38041 Grenoble.

Yann.Ourmieres@hmg.inpg.fr

Abstract

This study deals with the enhancement of an intermittent assimilation method applied to an Ocean General Circulation Model (OGCM). A major drawback of sequential assimilation methods is the discontinuity between the model forecast and the data assimilated state estimates due to the suboptimal processing of the intermittent approach. The data assimilation step, named the analysis step, is known to induce shocks in the model restart phase, causing spurious high frequency oscillations and data rejection. A method called Incremental Analysis Update (IAU) is now recognized to efficiently tackle these problems. The IAU methodology is detailed and the different schemes are discussed. An IAU scheme is chosen and implemented to an intermittent data assimilation system, using a low rank Kalman filter (SEEK), in the case of the OGCM OPA 8.1 set for ocean state prediction in the North Atlantic basin with a 1/3° grid resolution (NATL3 configuration). A one year (1993) experiment has been conducted for three different set-ups: the first test is a free run of the model without data assimilation, the second test is a run with intermittent data assimilation using the SEEK filter and the third test is an IAU implemented run. Results from all the runs are then compared, with a specific interest on high frequency output behaviors and solution consistency. The improvements brought up by the IAU implementation such as the disappearance of spurious high frequency oscillations and the time continuity of the solution are shown. An overall assessment of the impact of this new scheme on the assimilated runs is discussed. Advantages and drawbacks of the IAU method are pointed out. Finally, some possible improvements, mainly based on modifications of the IAU methodology, are revealed.

1. Introduction

Operational ocean prediction systems are developed for several purposes. Among them, providing short-range forecasts, ocean current hindcasts, estimations of the thermodynamic ocean state for seasonal and climate prediction and retrospective analyzes by the combination of data and model outputs can be considered as the main goals. By combining model estimates and observations, data assimilation systems aim at systematically evaluate theoretical model outputs with respect to reality, in order to improve modeling and observing systems. For such a difficult task, complex numerical models and assimilation methods are needed to optimize the use of spatially and temporally sparse observations. In order to produce the best possible forecast, the models have to be initialized with the most accurate ocean state available at eddy resolving resolution. Due to the chaotic nature of ocean dynamics, current models cannot predict the ocean state further than a certain time range. For

this reason, models need to be intermittently re-initialized by correcting the forecast with recent observations. In order to get the best possible update from the data, observations and model outputs reliability have to be assessed in terms of error estimation. Among the possible data assimilation methods, the optimal statistical estimation theory and more precisely the Kalman filtering approach is appropriate to supply a solution of the best linear unbiased estimation. Sequential filtering methods have been extensively studied and used for several years.

The main drawback of sequential methods is the discontinuity between the forecast and the analysis estimates due to the suboptimal processing of the intermittent approach. This discontinuity is recognized as a major problem. It can introduce a shock in the model restart stage, causing spurious high frequency oscillations, and possibly leading to data rejection. The transient waves introduced by the analysis step can be considered as the result of imperfect corrected ocean states, due to physically unbalanced error covariances.

In order to tackle these problems, Bloom et al. (1996) have proposed an algorithm called Incremental Analysis Update (IAU), consisting in incorporating the analysis increment in a gradual manner. The following subsections provide an overview of the different IAU methodologies applied to atmospheric and ocean circulation models. The principal characteristics of the IAU methodology are explained and discussed.

a. Atmospheric General Circulation Models (AGCM)

The IAU method was previously designed for intermittent data assimilation systems in atmospheric circulation models to reduce analysis-induced initial shocks in the model forecast. Bloom et al. (1996) were the first to introduce the IAU concept in data assimilation system within the Goddard Earth Observing System (GEOS). The basic principle of IAU is to incorporate an increment calculated from the analysis in the model integration as a forcing term. As mentioned by Bloom et al. (1996), the IAU procedure has the properties of a low-pass time filter and can then help in reducing high frequency oscillations often observed at the restart of the model after the analysis step.

A schematic overview of the IAU procedure as described by Bloom et al. (1996) is shown in figure 1. In the particular case of Bloom et al. (1996), the assimilation process is restarted 3h before the analysis step and the model is integrated forward for 6h with the IAU forcing. At the end of the IAU forcing run, the model performs a free run for a period of 3h, providing the first guess for the next analysis. In this case, the IAU increment is constant through the IAU forcing time window. For the analysis step only past data are used.

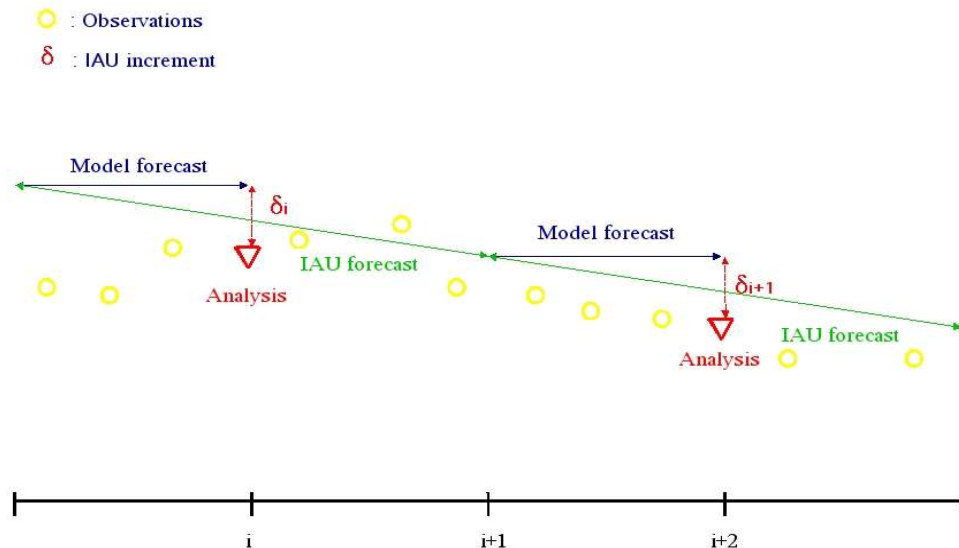


Figure 1: IAU method from Bloom et al.(1996).

The IAU procedure is widely used in atmospheric models and mainly in a similar way to Bloom's description (Schubert et al. 1993, Zhu et al. 2003, DeWeaver et al. 1997). This method has been acknowledged to feature several advantages in the model integration process. As mentioned by Bloom et al. (1996), it acts like a continuous assimilation method (cf. Fig. 1). It also controls imbalances introduced by the analysis step (Zhu et al. 2003). It suppresses gravity waves due to assimilation update, minimizing spurious adjustment processes (DeWeaver et al. 1997).

In a recent work from Polavarapu et al. (2004), comparisons between IAU and Incremental Digital Filtering (IDF) are made leading to several interesting points. They stated that the IAU response does not depend only on the waves frequency but also on the model dynamics, therefore the waves growth rate is of influence too. Polavarapu et al. (2004) also concluded that the IAU could damp slower waves too much when a constant increment is applied. In addition to that they stated that fast waves could also be insufficiently damped.

b. Ocean General Circulation Models (OGCM)

Compared to its use in atmospheric models, the IAU procedure has only been implemented into ocean circulation models quite recently. The main targeted goals when applying such a method are globally the same as the ones previously described for atmospheric models. However, different methods have been developed and applied to OGCM, although the overall principles remain similar. Carton et al. (2000) have adapted a technique very close to Bloom's method, the main difference being the duration of the model forecast and the IAU forcing time window, due to the different time scales of the ocean dynamics. The model is run for 5 days, followed by an analysis and the increment calculation. In this case, the increment is correcting the mass fields. Then the model restarts 5 days prior to the analyzed time and performs an IAU run, forced with the increment, for 10 days. The initial conditions for the next five-days forecast are then provided by the state obtained at the end of the IAU incremental forecast. According to Carton et al. (2000), this method have both advantages of acting like a continuous assimilation method and suppressing gravity waves induced by the analysis update process. Moreover, Carton et al. (2000) also

stated that because of this continuous correction of the forecast, the effect of the bias was reduced on the analysis. On the other hand, the cost of this technique is a 50% increase in integration time over that of a usual 10-day intermittent assimilation scheme.

Huang et al. (2002) developed a different IAU methodology, computationally more economical than the Bloom's version. For this study, the model used is a version of the GFDL Modular Ocean Model (Pacanowski et al., 1993) and the assimilation system is the Ocean Data Assimilation (ODA) system (Derber and Rosati, 1989). With this ODA configuration, the temperature correction is inserted into the model for twelve hours. At the end of this twelve hours run, a temperature increment is calculated and applied at every time step for the next twelve hours. This persistent method was developed by Rosati et al. (1995). Huang et al. (2002) also tested a modified strategy: a temperature increment is calculated from an analysis done after one hour of model prediction. This increment is divided by the number of time step in a day (24 in this case) and converted into a 24 hours time tendency. This tendency will then be added to the model temperature field, at each time step, including the one from which the increment has been derived, for a 24 hours forecast. According to Huang et al. (2002), such a method still preserves model internal fluctuations while damping analysis-induced high frequency signals. By studying further some results obtained with this new methodology, they also claim that a non-assimilated variable such as the velocity could give a closer agreement with observational data than the former strategy from Rosati et al. (1995) would do. It is important to note that the determination of a non-assimilated variable is dependent on the dynamical coupling between variables, hence its quality can reveal how the observational and dynamical data are balanced in the assimilation scheme.

In Alves et al. (2004), the temperature observations are assimilated into the ocean model as it is integrated. Every ten days, an analysis is done using observations five days before and after the analyzed time. An increment is calculated from the difference between the analyzed and the forecast state. This increment is then added to the temperature field integration for the subsequent ten days. The model state obtained is then used for the next analysis step. As shown in figure 2, the major difference with other methods is that the incremental integration is continuous as no model forecast without IAU forcing is performed. Besides, compared to other techniques, no change is made to the salinity field.

A procedure similar to Alves et al. (2004) is used in Weaver et al. (2003), for their three dimensional variational assimilation system developed for the OPA model. Their analysis only produces an increment for the temperature field and this increment is applied as a constant forcing through the time window.

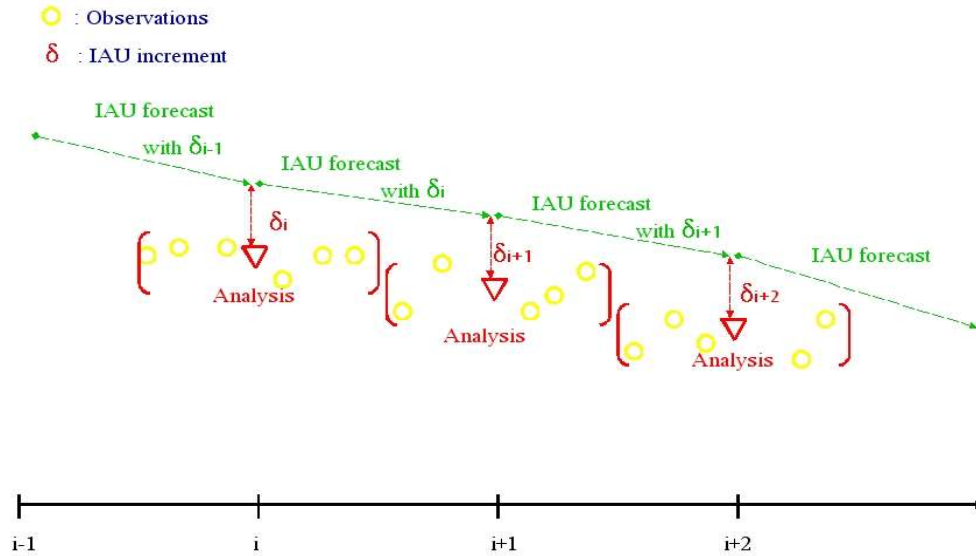


Figure2: IAU method from Alves et al.(2004).

c. Discussion

From a review on relevant work using IAU, several key ideas can be pointed out. The method itself is not unique as major differences exist, especially when applied to ocean general circulation models. Differences between the methodologies used in Carton et al. (2000), Huang et al. (2002) and Alves et al. (2004) mainly stand in the increment calculation and the choice in its time-window application. However, all authors agree on the benefits of the IAU implementation. It offers the advantage of a continuous assimilation method, while providing a reduction of analysis-induced oscillations. Another recognized upside is a reduction of the bias impact as the model forecast is constantly corrected.

Nevertheless, it is important to note that IAU implementation will always increase the computing time depending on which scheme is used. In addition to that Polavarapu et al. (2004) also stated a few drawbacks for the IAU impact such as a possible damping of slower waves and an insufficient damping of some faster waves in some cases.

Next sections of this work focus on the specific IAU implementation and its overall behavior, using the facts presented in this introduction.

2. Model configuration and IAU implementation

a. Model configuration

The numerical code used is OPA 8.1, a z-coordinate, primitive equation model using the hydrostatic approximation and the rigid lid condition. Extended information on OPA8.1 can be found in Madec et al. (1998). The state vector includes the horizontal velocity U , the vertical velocity V , the temperature field T , the salinity field S , and the barotropic stream function BSF as in Testut et al. (2003).

The grid configuration is the NATL3 configuration, featuring a model domain covering the North Atlantic basin from 20° S to 70° N and from 98.5° W to 20° E

with a horizontal resolution of $1/3^\circ \times 1/3^\circ \cos(\text{latitude})$. The vertical discretization is done on 43 geopotential levels, with a grid spacing increasing from 12 m at the surface to 200 m below the depth of 1500 m.

b. Data assimilation scheme

The analysis scheme is a reduced-rank Kalman filter derived from the Singular Evolutive Extended Kalman (SEEK) methodology (Pham et al., 1998). This sequential method has been described and used in several studies (Brasseur et al., 1999, Brankart et al., 2003, Testut et al., 2003). The overall analysis process is similar to the one explained in Testut et al. (2003). The estimation vector contains the variables on which statistical analysis is done and includes the zonal velocity U , the meridional velocity V , the temperature field T , the salinity field S , the Sea Surface Height SSH. The control vector contains the variables used to constrain the model and includes (U, V, T, S).

The data assimilated are the Sea Surface Temperature SST, the SSH and the Sea Surface Salinity SSS. The SST data set consists of AVHRR observations gathered in the NASA pathfinder project remapped at a $1/4^\circ$ resolution with a time periodicity of 10 days. The SSS data set is derived from the Levitus monthly climatology (Levitus et al., 1998). The SSH data set consists of a combination of Topex/Poseidon and ERS altimeters along track data for the period December 1992 to December 1993.

c. IAU methodology

An original IAU method has been chosen using information provided by the diverse approaches cited in section 1. All the tests and results presented in this study were done using the configuration illustrated by figure 3. The method can be described as follows: a model forecast is done from time i to $i+1$ and an analysis is performed at time $i+1$. An increment is calculated on the temperature and salinity fields by taking the difference between the analyzed and the forecast fields. Then the model is run again from time i to $i+1$, but with the increments applied to the corresponding fields. During this IAU forecast, the additional forcing term imposed to the model salinity and temperature fields at each time step is a fraction of the increment. In the present case, as in most IAU methodologies, this forcing term is the increment divided by the duration of the assimilation cycle Δt_c (cf. Equations 1 and 2). Hence, this value is constant during the IAU forecast and the time-integrated quantity of this value over the IAU forcing time window is the increment. The obtained state at $i+1$ will then provide the initial conditions for the next model forecast. This particular method was chosen because of the convenient modifications needed to be done in the model and also because it offers the possibility to compare the forecast, the analyzed and the IAU corrected states at the same time. However, compared to the method from Bloom et al. (1996), only increasing the cpu time of 50%, the present method leads to an increase in the integration time of the model of 100%.

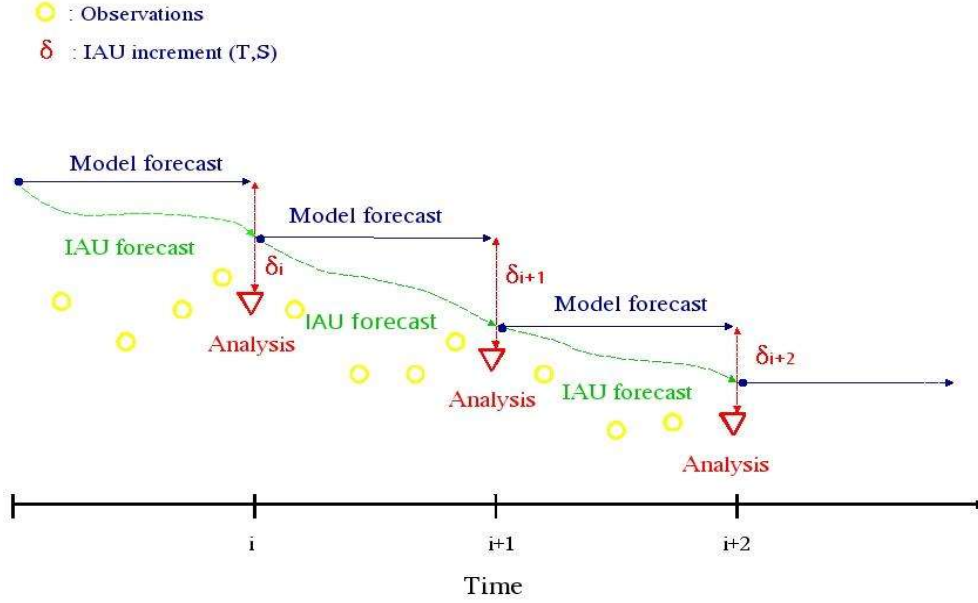


Figure 3: IAU configuration used for the present study.

During the IAU forecast, the increments δT_{IAU} and δS_{IAU} are applied as shown in equations (1) and (2):

$$\frac{\partial T}{\partial t} = -\nabla \cdot (T \mathbf{U}) + D^T + \lambda(t) \delta T_{IAU} , \quad (1)$$

$$\frac{\partial S}{\partial t} = -\nabla \cdot (S \mathbf{U}) + D^S + \lambda(t) \delta S_{IAU} , \quad (2)$$

with \mathbf{U} the vector velocity, D^T and D^S the parametrizations of small scale physics for temperature and salinity including the surface forcing terms and $\lambda(t)$ a parameter such that

$$\int_0^{\Delta t_c} \lambda(t) dt = 1 \quad (3)$$

with Δt_c the duration of the assimilation cycle. In the present case $\lambda(t)$ is chosen to be constant:

$$\lambda(t) = \frac{1}{\Delta t_c} . \quad (4)$$

The control vector in the IAU configuration is (T, S), it is then different from the control vector of the presented intermittent assimilated run. It is important to note that the incremental update value applied to T and S for a given grid point is constant through the IAU forcing assimilation cycle. Applying a constant value for the increment is the method mostly used, however Polavarapu et al. (2004) stated that a the IAU response in such a case might damp slower waves too much.

It is important to note that the incremental correction could be applied to other variables such as the horizontal velocities U,V. Additional tests not discussed in the present study showed that a correction on the horizontal velocities along with the correction on T and S could also produce satisfying results. The choice of the variables to be corrected remains a difficult issue. However, most of the work with OGCM, presented in section 1.b, was conducted with corrections applied on T and S. As a result, the choice of a T,S correction in the present study was influenced by the

work previously conducted with IAU implementation but also by the fact that testing the correction effects seems more convenient and objective for fewer than a large number of variables.

3. The conducted experiments

Numerical experiments have been conducted using the model configuration, the assimilation method and the IAU technique described in section 2. In order to get relevant comparisons with the IAU implemented tests, experiments for similar time periods have been systematically repeated for the case of a model free run, without data assimilation, and for the case of a run with regular intermittent data assimilation. As a result, this study features results from three different configurations ran over the same time period: a free run, a classic intermittent run with data assimilation and an IAU implemented run.

For these three types of run, the outputs have been cautiously done for similar dates and locations. The experiments have been conducted for a period of one year, starting from the 4th of December 1992 and ending the 5th of December 1993. All the state vector fields are saved every day. Six grid points have also been selected, for which high frequency outputs (every time-step) are done for the temperature, the salinity and the SSH. These points have been arbitrary selected but chosen to correspond to areas of interesting ocean activity. Four of these points also correspond to locations of real moorings taken from the WOCE database(ACM25/26 campaigns, 1993), that were operational during the same period, providing an independent data set of temperature and salinity values. Table 1 is a summary of the points characteristics while figure 4 shows the point locations in the North Atlantic basin.

<i>Point number</i>	<i>Latitude N</i>	<i>Longitude W</i>	<i>Mooring</i>
1	18	34	Yes
2	26	29	Yes
3	33	22	Yes
4	26	79	Yes
5	35.5	66.3	No
6	60	30	No

Table 1: High-frequency points characteristics.

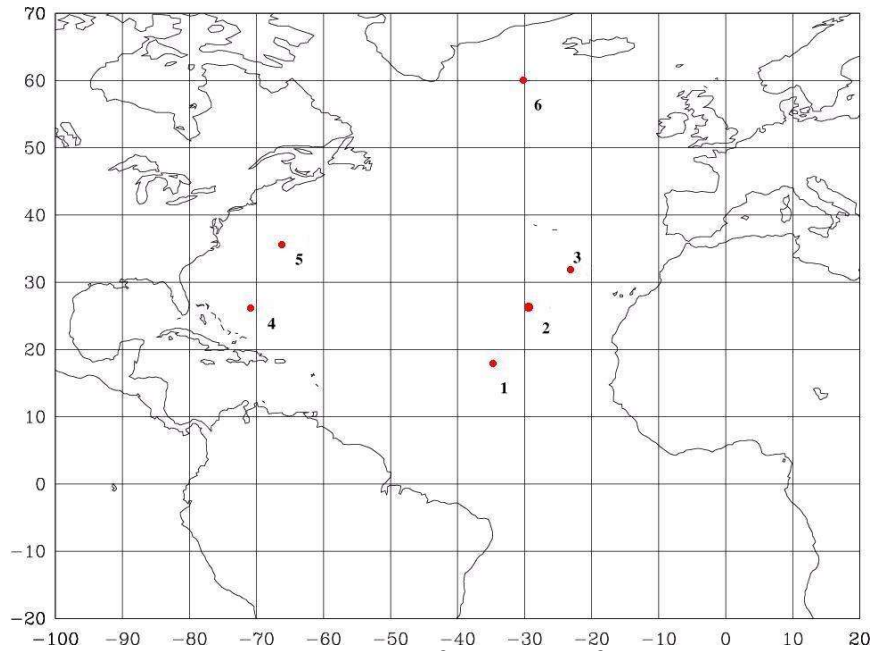


Figure 4: Grid point locations for the high frequency outputs.

The time step of the model being 40 minutes, the output from the model evolution of the temperature, salinity and SSH at the six selected grid points will then be produced 36 times per day.

Concerning the data assimilation characteristics, an analysis was performed every three days for the classic intermittent experiment and the IAU implemented experiment. Therefore, according to figure 3, in the IAU configuration, the model performs a forecast from day 0 to day 3, then an analysis is done at day 3. The increments are calculated from the difference between the forecast and the analyzed states at day 3, then an IAU forecast with incremental forcing is done from day 0 to day 3. The IAU state obtained at day 3 is further used as the initial state for the model forecast from day 3 to day 6, and so on.

4. Results

As shown in section 1, implementing an IAU method aside with the assimilation process is usually done for two reasons: first, it is supposed to suppress spurious high frequency oscillations on the variable trajectories and second it should provide a time continuous solution. This section shows advances brought up by the IAU method in these two areas along with additional results on the general behavior and efficiency of the model fully set with the IAU method and the assimilation process when compared to the model free run and the model run with intermittent data assimilation. From now on, for reading convenience, the model run including the IAU method and the assimilation process will be named “IAU run”, the free model run will be named the “FREE run” and the model run with intermittent assimilation method will be named “INT run”.

a. High frequency oscillations

1) Oscillation filtering

When the model output for a few selected grid points (cf. section 3) is considered, it is shown that, at least for the output variables (temperature, salinity and SSH), high frequency oscillations are a common feature of the INT run but when the IAU run is considered, these oscillations are strongly damped or completely missing indeed.

Figure 5 shows the SSH evolution for a period starting from December the 4th, 1992 to December the 5th, 1993 for the INT run and the IAU run for the grid point 3, located in the Portugal current area. Despite having a trajectory not always similar to the INT one, the IAU trajectory does not feature the high frequency oscillations clearly noticeable for the INT run.

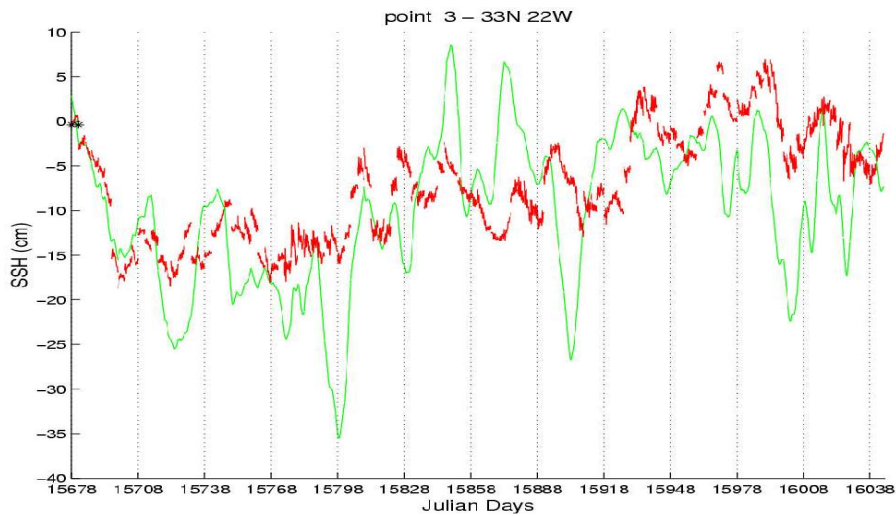


Figure 5: High frequency evolution of the SSH (cm) for grid point 3 during a year.

- INT run, - IAU run. X-axis is the time in Julian days(starting from 01/01/1950):
15678 is 04/12/92, 16038 is 29/11/93.

Figure 6 is a similar example of high frequency damping with the IAU implementation but for the SST at the grid point 5, located in the Gulf Stream region. This kind of oscillation has been noticed for all the variables studied at single grid point locations. The periodicity of these oscillations could not be clearly identified, varying from one point to another, as well as from one variable to another. The estimated periods of oscillations fluctuate between 12 hours to nearly 3 days, with a strong component centered on 24 hours.

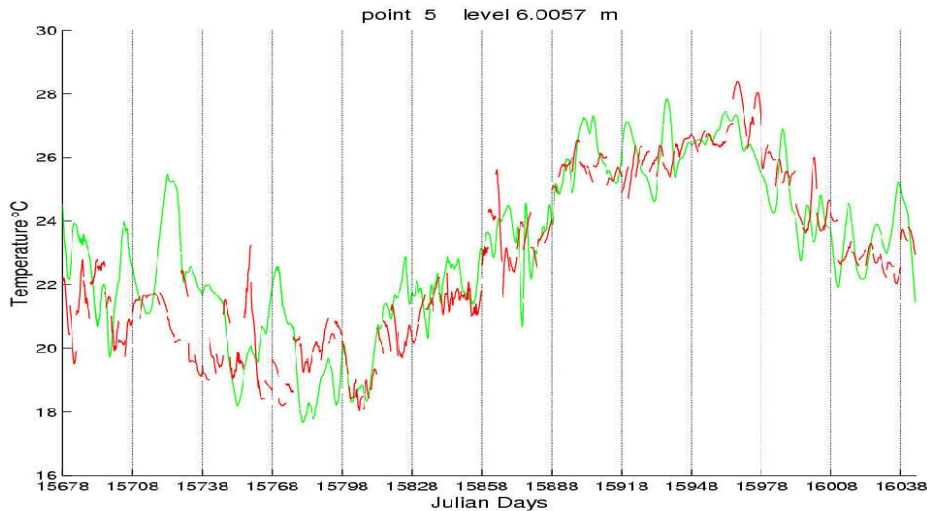


Figure 6: High frequency evolution of the SST ($^{\circ}$ C) for grid point 5, during a year.
 - INT run, - IAU run. X-axis is the time in Julian days: 15678 is 04/12/92, 16038 is 29/11/93.

If a Gulf stream region is defined as shown in figure 7, spatially averaged fields can be calculated and their evolution can be seen on a daily base, as all the runs were also set to output the state vector fields every day.

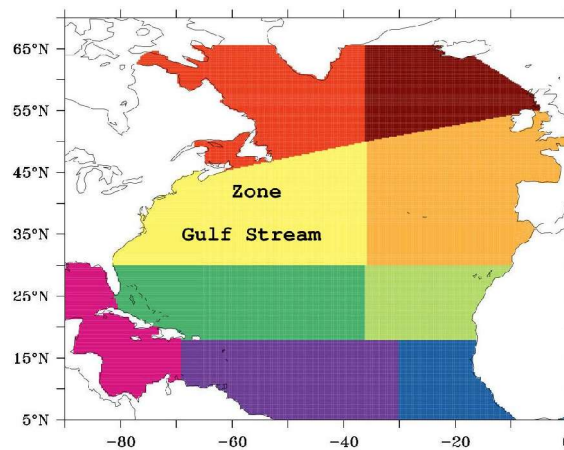


Figure 7: Gulf Stream zone used for spatial average calculations (in yellow).

Figure 8 is an example of the daily evolution of the horizontal velocity U at a depth of 55 m, when a spatial average is done on the Gulf Stream zone defined in figure 7, for the case of the IAU and INT run. Despite considering a spatial average over a large region, spurious oscillations are still noticeable for the INT run, while they clearly appear to be strongly damped for the IAU run. The period of the spurious large amplitude oscillations has changed compared to that of the single grid points (cf. Fig. 5 and 6), and can be identified here as nearly 3 days, corresponding to an assimilation cycle length.

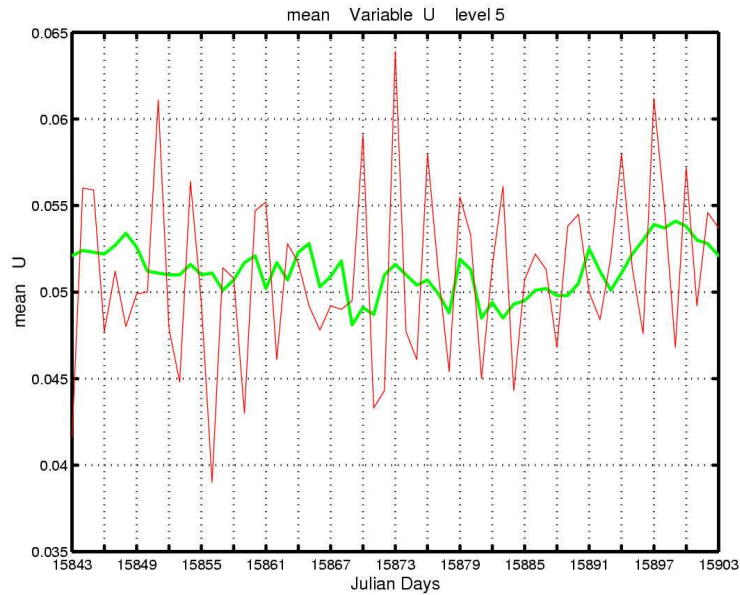


Figure 8: Daily evolution of the spatially averaged horizontal velocity U in the Gulf Stream zone at a 55 m depth (model depth level 5); - INT run, - IAU run; X-axis is the time in Julian days: 15843 is 18/05/93, 15903 is 17 /07/93.

In figure 9, the evolution of the spatially averaged SST in the Gulf Stream zone is plotted for a year, and the IAU, the INT and the FREE run are compared.

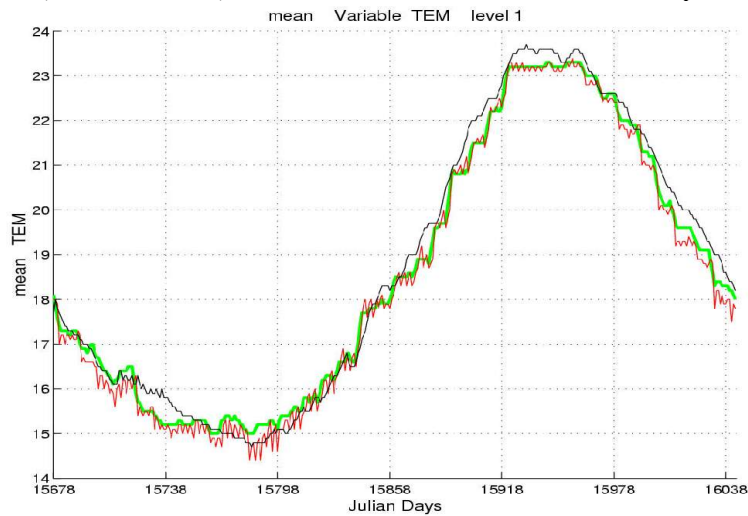


Figure 9: Daily evolution of the spatially averaged SST in the Gulf Stream zone;- FREE run, - INT run, - IAU run; X-axis is the time in Julian days: 15678 is 04/12/92, 16038 is 29/11/93.

As in figure 8, despite the spatial average, the INT run still features oscillations, lasting throughout the entire year, and appearing to be significantly damped in the IAU run. The overall solution remains similar for the IAU, INT and FREE runs, describing a strong seasonal cycle.

2) Signal filtering and alteration

As mentioned by Polavarapu et al. (2004), the IAU procedure can affect the overall signal by damping too much low frequency waves. Figure 10 shows the evolution of

the horizontal velocity U spatially averaged in the Gulf Stream zone at a depth of 55 m, for the usual period of a year. As can be seen in figure 10, for a period running from December 1992 to April 1993 (around Julian day 15798), the FREE run exhibits large amplitude oscillations, satisfyingly reproduced in the IAU run. Then for a period of 6 months (approximately until early October 1993, around Julian day 15978), the FREE run oscillation amplitudes significantly weaken and so do the oscillations in the IAU trajectory, but extensive amplitude oscillations are still present for the INT run. As soon as the FREE run large amplitude oscillations restart at the end of year 1993, the IAU trajectory will again include similar oscillations. Such a result confirm that the overall signal when featuring significantly large waves does not seem to be filtered out by the IAU method. On the other hand, the spurious oscillations included in the INT run are clearly damped by the IAU method. In this case, the periodicity of the FREE run oscillations is about 4 days and more, being quite close to the main periodicity of the INT oscillations, estimated as nearly 3 days. It turns out that the frequency of the oscillations might be less important than the model dynamics, from the IAU impact point of view, as the oscillations are not filtered out when they are apparently part of the model dynamics and the oscillations simply vanish when they seem to be part of a spurious effect, despite being of similar order of periodicity in this case.

These considerations do not agree very well to Polavarapu et al. (2004) as no obvious weakening of the overall signal could be witnessed in the present experiment, however they did mention this effect mostly for waves of periods longer than the ones discussed here. In section 4.e, it is also demonstrated that no such problem could be pointed out when the Root Mean Squared (RMS) differences between the assimilated data and the IAU forecast are considered.

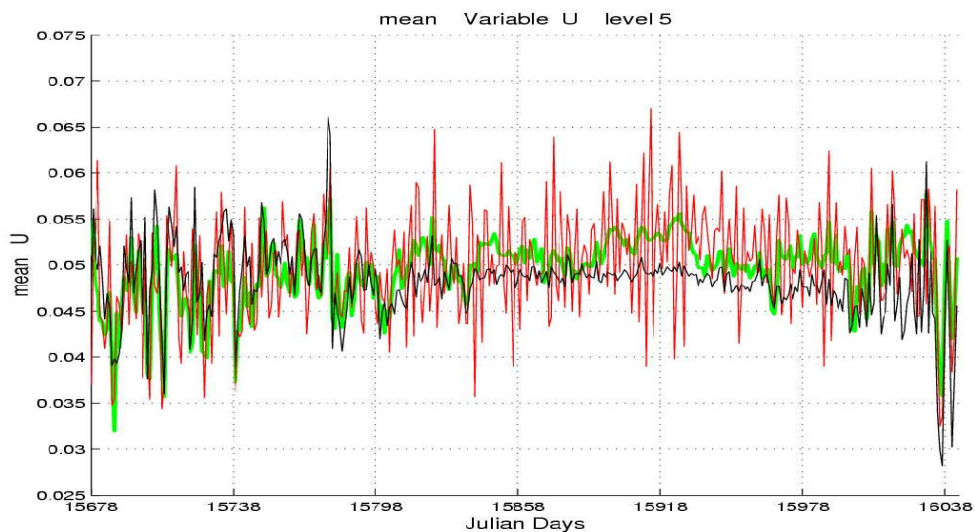


Figure 10: Daily evolution of the spatially averaged horizontal velocity U in the Gulf Stream zone at a 55 m depth (model depth level 5); - FREE run, - INT run, - IAU run; X-axis is the time in Julian days: 15678 is 04/12/92, 16038 is 29/11/93.

3) Spurious trajectories at isolated grid points

Among the numerous results obtained with these experiments, the high frequency outputs showed various outcomes. Despite the obvious high frequency oscillation filtering properties of the IAU detailed in the previous subsections, some surprising peaks in the IAU trajectory have been noticed in a few cases. These peaks do not

behave like oscillations afterwards but their occurrence seems peculiar. Figure 11 shows the temperature increment δT_{IAU} evolution for 24 assimilation cycles (of 3 days each), while figure 12 shows the SST evolution for the same period obtained for all the runs for the grid point 5. It seems that the SST trajectory from the IAU run reacts well to the increment variations, with a short time delay. It is however not clear why the increment is subjected to this kind of large amplitude peak from one cycle to another, but the fact that the trajectory is studied at a single grid point is probably determinant in the occurrence of such events. For example, a small shift in the position of an eddy in the Gulf Stream region from one assimilation cycle to another, can lead to a huge difference between the previous and the new increments. Consequently, if a larger domain is integrated, no such difference would occur. Hence, when an entire ocean region is of interest, this type of peak systematically vanish, as shown in figure 8.

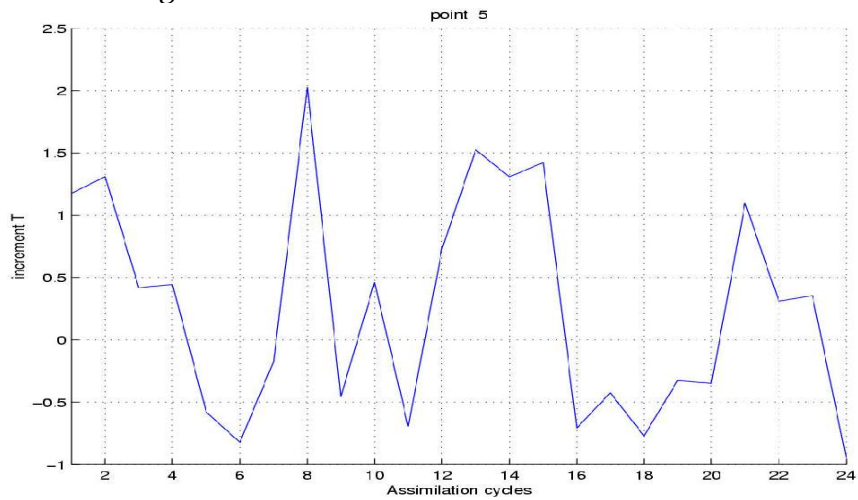


Figure 11: IAU temperature ($^{\circ}\text{C}$) increment δT_{IAU} evolution for 24 assimilation cycles for grid point 5 (Gulf Stream region). Period: 07/12/92 to 14/02/93.

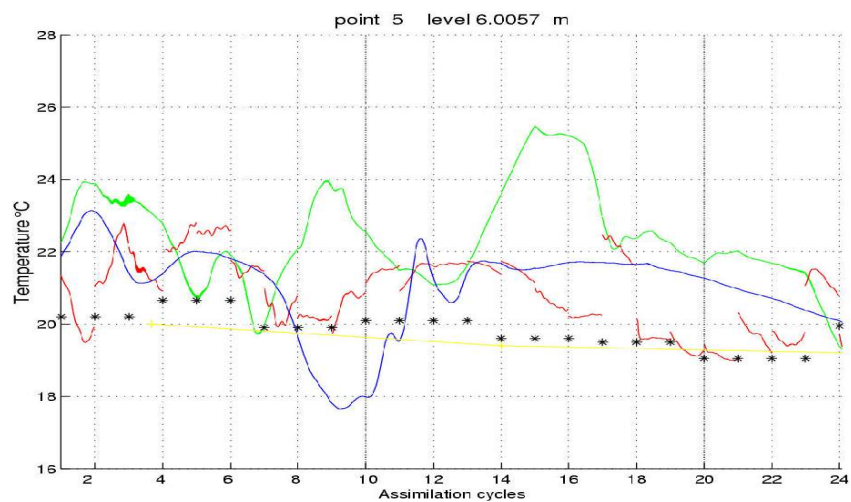


Figure 12: SST evolution ($^{\circ}\text{C}$) for 24 assimilation cycles for grid point 5 (Gulf Stream region); period: 07/12/92 to 14/02/93; - FREE run, - INT run, - IAU run, * Assimilated data, - Levitus (1998) climatology. X-axis is the time in assimilation cycles.

4) oscillations duration

Additional tests have been performed to study the duration of the oscillations shown in section 4.a.1. In order to do so, the ocean states obtained after nine months of experiments in the case of the INT run and the IAU run have been selected. Two free model forecasts have been run starting from these two different states. If the temperature trajectory for isolated grid points is plotted out, results show that the oscillations existing in the intermittent run can last more than 15 days, as illustrated in figure 13. If the SSH trajectory is of interest, it turns out that oscillations can last over the entire month, as shown in figures 14 and 15. If spatially averaged values of the horizontal velocity U are considered for the Gulf Stream zone (cf. Fig 7), oscillations still last over a month for the case of the free run restarted from an ocean state obtained with intermittent assimilation, as shown in figure 16. From these results, a striking note can be made concerning the effect of the IAU increment on the model solution. However the IAU method is known to suppress high frequency oscillations, it turns out that a free run started from an ocean state obtained after several months of IAU forecast does not feature any oscillations, when a free run started from an ocean state obtained after a similar period but with intermittent assimilation will exhibit spurious oscillations lasting several weeks. It may then be that the ocean states obtained after several months of IAU forecast are more balanced.

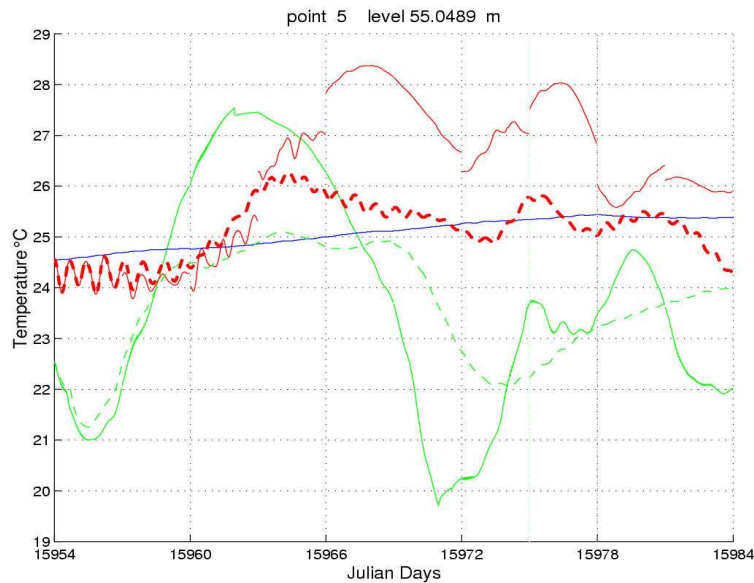


Figure 13: High frequency evolution of the temperature T ($^{\circ}\text{C}$) for grid point 5 (Gulf Stream region) at a depth of 55 m . - FREE run, - INT run, - IAU run, - - free run started from an INT obtained state, - - free run started from an IAU obtained state. X-axis is the time in Julian days: 15955 is 07/09/93, 15984 is 06/10/93.

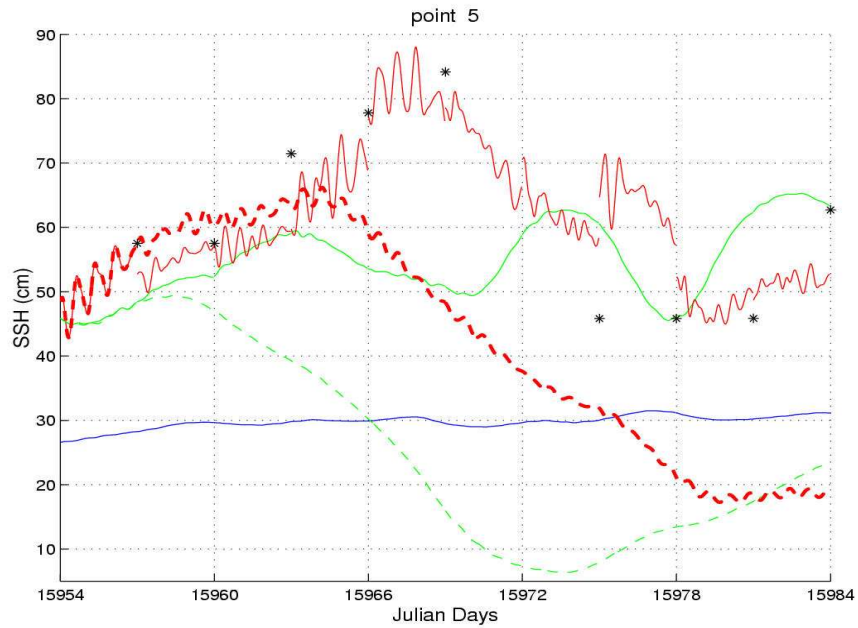


Figure 14: High frequency evolution of the Sea Surface Height (cm) for grid point 5 (Gulf Stream region). - FREE run, - INT run, - IAU run, - - free run started from an INT obtained state, - - free run started from an IAU obtained state, * Assimilated data. X-axis is the time in Julian days: 15955 is 07/09/93, 15984 is 06/10/93.

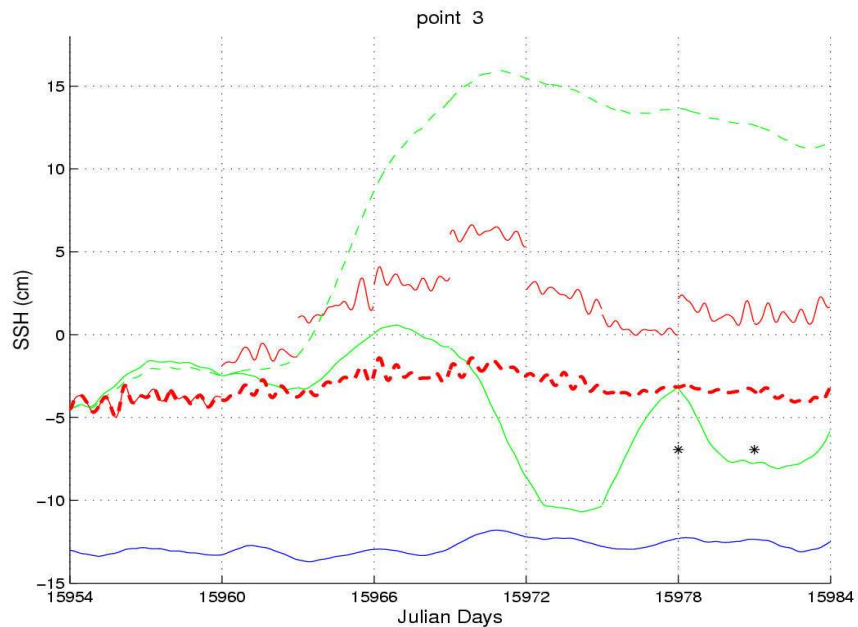


Figure 15: High frequency evolution of the Sea Surface Height (cm) for grid point 3 (Azores current region). - FREE run, - INT run, - IAU run, - - free run started from an INT obtained state, - - free run started from an IAU obtained state, * Assimilated data. X-axis is the time in Julian days: 15955 is 07/09/93, 15984 is 06/10/93.

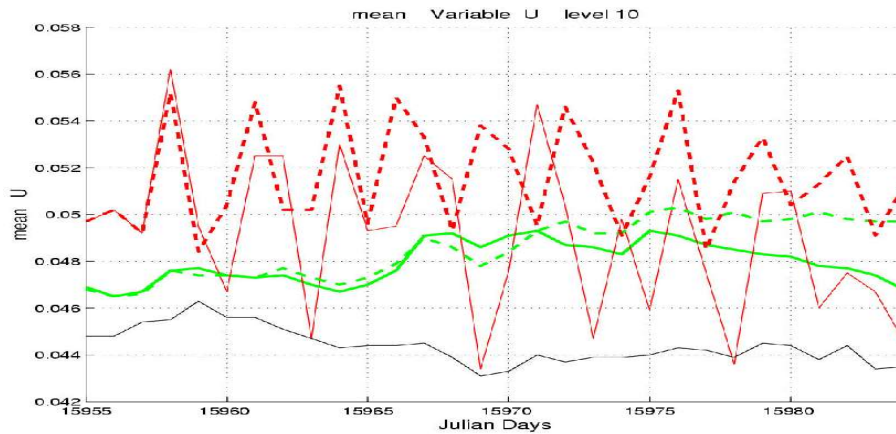


Figure 16: Evolution of the spatially averaged horizontal velocity U (m/s) for the Gulf Stream zone at a depth of 130 m. - FREE run, - INT run, - IAU run, - - free run started from an INT obtained state, - - free run started from an IAU obtained state. X-axis is the time in Julian days: 15955 is 07/09/93, 15984 is 06/10/93.

b. Time continuity

A great asset of the IAU methodology is that it provides a continuous solution. Figure 6 (section 4.a.1) simply illustrates the continuous trajectory of the SST for the case of an isolated grid point in the Gulf Stream region when compared to the equivalent trajectory obtained by intermittent data assimilation. Figure 17 is a similar example but for a grid point located in the Portugal current.

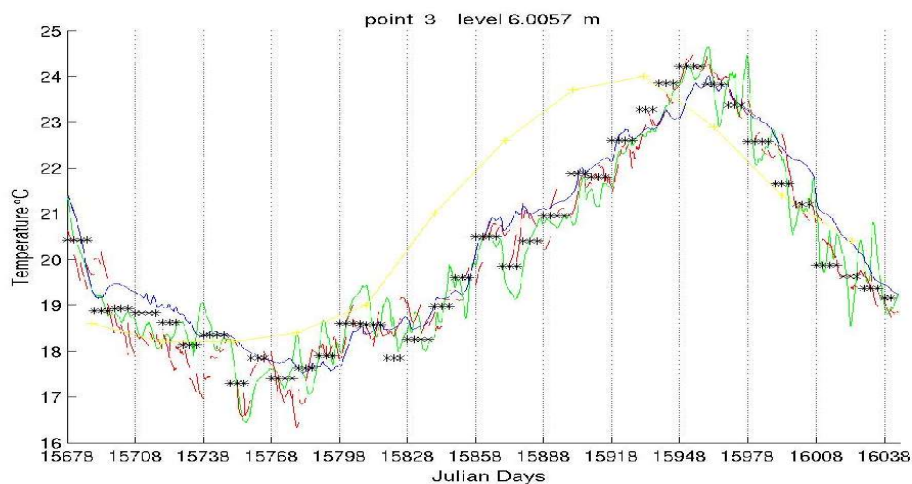


Figure 17: High frequency evolution of the SST ($^{\circ}$ C) for grid point 3, for. - FREE run, - INT run, - IAU run, * Assimilated data, - Levitus (1998) climatology. X-axis is the time in Julian days: 15678 is 04/12/92, 16038 is 29/12/93.

Figure 17 clearly demonstrates that the IAU technique acts as a continuous assimilation method by opposition to the discontinuous trajectory of the INT run. It can also be noted that the IAU solution matches quite closely the assimilated observations.

c. RMS difference with the assimilated data

As described in the previous sections, the IAU technique delivers good results when suppressing spurious waves and obtaining a continuous solution are of interest. Nevertheless, in order to validate such a method, it is also important to study the overall performance of the IAU implementation in terms of Root Mean Squared differences between the assimilated observations and the IAU forecast. Figure 18 shows the RMS obtained for the SST over the entire North Atlantic basin for the FREE run, the INT run and the IAU run for a year.

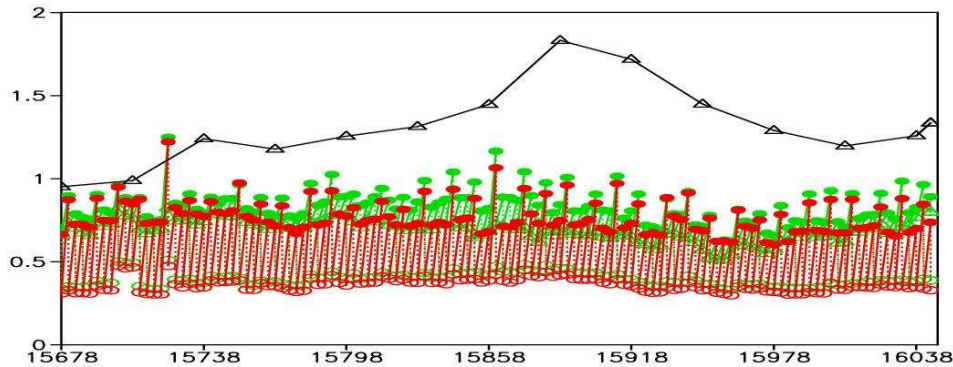


Figure 18: RMS differences with the assimilated data for the SST (entire basin); $-\Delta$ - FREE run; \bullet forecast in INT mode, \circ analysis in INT mode; \bullet forecast in IAU mode, \circ analysis in IAU mode, Δ forced forecast in IAU mode.

From figure 18, it appears that for the RMS on the SST, neither the analysis nor the forecast for the IAU mode can be considered as unsatisfactory compared to their equivalent for the INT run. The RMS values of the forced forecast in IAU mode are also systematically smaller than the RMS values of the INT forecast. When the RMS obtained for the SSH over the entire basin is plotted for the three types of run (figure 19), results are quite different.

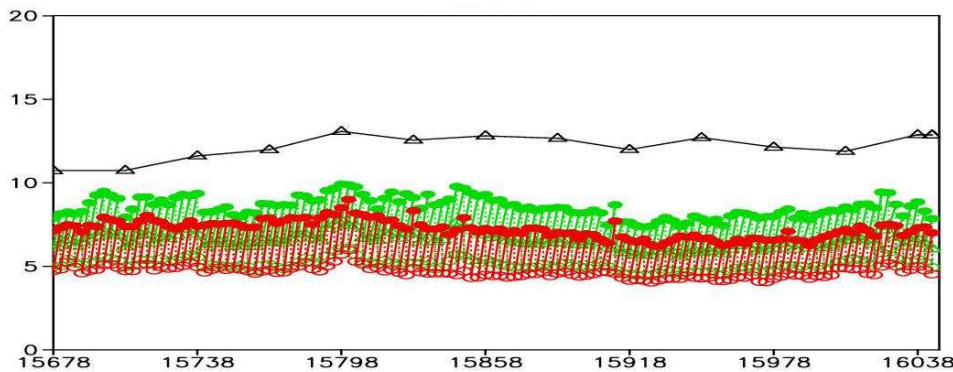


Figure 19: RMS differences with the assimilated data for the SSH (entire basin); $-\Delta$ - FREE run; \bullet forecast in INT mode, \circ analysis in INT mode; \bullet forecast in IAU mode, \circ analysis in IAU mode, Δ forced forecast in IAU mode.

In a similar way to the RMS on the SST, the RMS on the analyzes for both cases INT and IAU are of similar order, but the RMS on the forecast in IAU mode gives poor results. However, the RMS trajectory of the forced forecast in IAU mode is

continuously improved compared to the RMS on the forecast in INT mode. Such an outcome is difficult to diagnose as no direct correction is applied on the variable SSH. However, the analysis step is strongly influenced by the SSH data, therefore the increment itself incorporates information from the assimilated SSH data. Such a result remains consistent when the RMS is calculated for the selected zone of the Gulf Stream (cf. Fig. 7), as shown in figure 20.

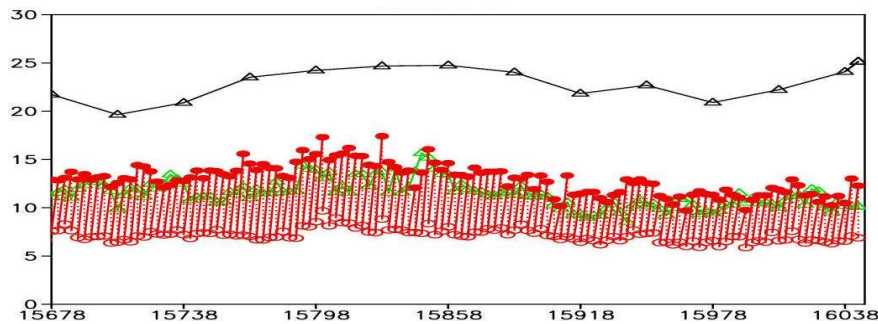


Figure 20: RMS difference with the assimilated data for the SSH (Gulf Stream zone); Δ - FREE run; \bullet forecast in INT mode, \circ analysis in INT mode; \blacktriangle forced forecast in IAU mode.

It appears that the RMS scoring of the IAU run is not unsatisfactory compared to the RMS calculated from the INT run, moreover a slight improvement is generally noticed. This also confirms the results discussed in section 4.a.2. concerning a possible signal alteration.

d. Spatial averaged field evolution

As shown in section 4.a.1., spatially averaged quantities have been calculated for the Gulf Stream zone (cf. Fig 7). This section focuses on the spatially averaged horizontal velocity evolution, at different depth. Figure 21 shows such a quantity at the sea surface while figures 22 and 23 are for depths of 452 m and 1045 m respectively. The similar quantity at a depth of 55 m is shown in figure 10 (cf. section 4.a.2). At the surface the averaged velocity from the FREE run, the INT run and the IAU run are nearly always superposed with few overshoots from the IAU or INT run. At a depth of 55 m, the agreement remains good between the runs, despite the large amplitude oscillations of the INT run discussed in previous section 4.a.2. At a depth of 452 m (Fig. 22), the INT and IAU trajectories start to drift away from the FREE run, with the INT run still featuring large amplitude oscillations, from the middle of the period considered, corresponding to early June 1993. Then for a depth of 1045 m (Fig. 23), this drift appears even clearer, triggered at the same time, but with an obvious strong drift of the IAU run compared to the INT run. This might come from the fact that no correction is applied to the ocean state after 1000 m in the case of the INT configuration, while the increment is applied throughout the entire depth for the IAU run (cf. section 4.e.). In addition to that, the similarity noticed for the surface current for the three runs (Fig. 21) probably comes from the fact that the surface currents are strongly driven by the wind. On the other hand, the differences between the free run and the assimilated IAU and INT runs for deeper velocities (Fig. 22 and 23) show that deeper currents are likely to be more influenced by data assimilation, as in the present case where the Gulf Stream characteristics are significantly modified.

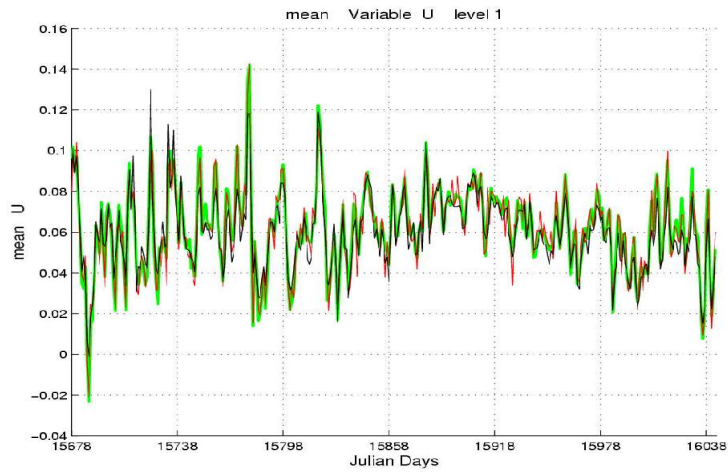


Figure 21: Daily evolution of the spatially averaged horizontal velocity U in the Gulf Stream zone at the sea surface (model level 1); - FREE run, - INT run, - IAU run; X-axis is the time in Julian days: 15678 is 04/12/92, 16038 is 29/11/93.

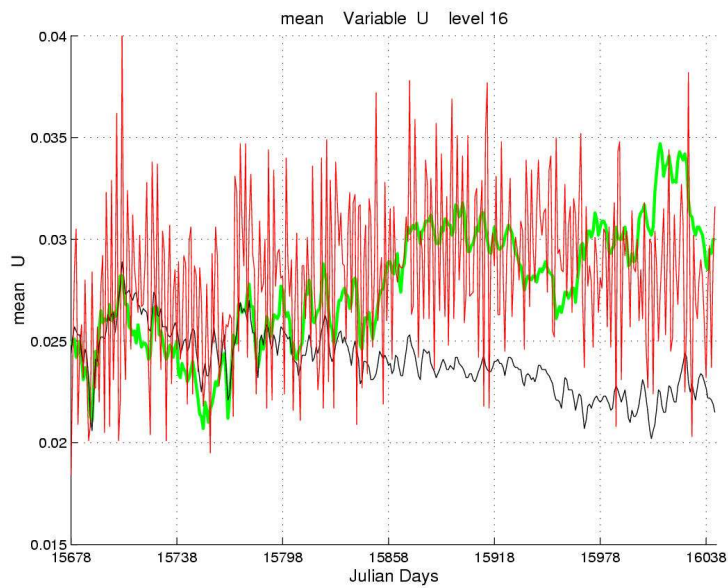


Figure 22: Daily evolution of the spatially averaged horizontal velocity U in the Gulf Stream zone at a depth of 452 m (model level 16); - FREE run, - INT run, - IAU run; X-axis is the time in Julian days: 15678 is 04/12/92, 16038 is 29/11/93.

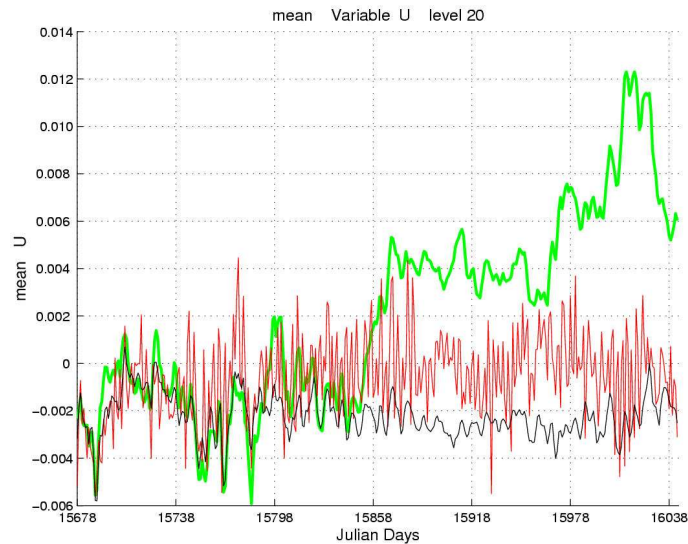


Figure 23: Daily evolution of the spatially averaged horizontal velocity U in the Gulf Stream zone at a depth of 1045 m (model level 20); - FREE run, - INT run, - IAU run; X-axis is the time in Julian days: 15678 is 04/12/92, 16038 is 29/11/93.

e. Global EKE production

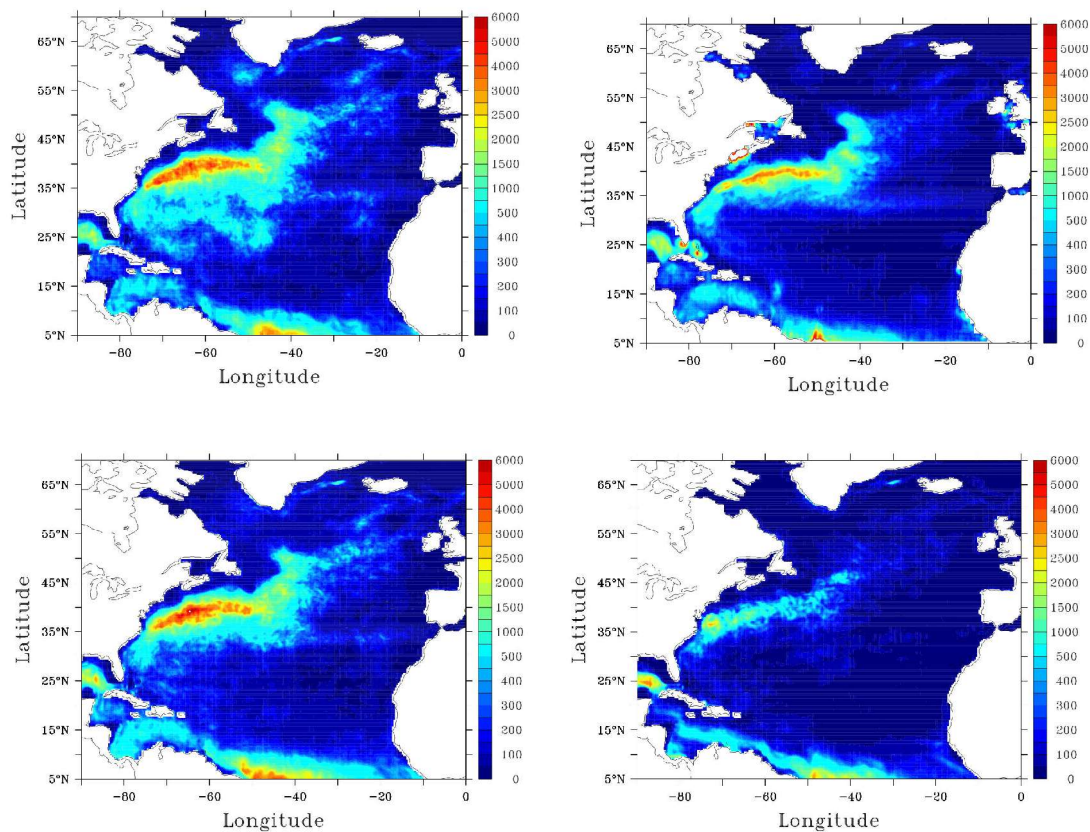


Figure 24: EKE (cm^2/s^2) calculated for the period 04/12/92 to 05/12/93, except top right caption, at the sea surface. Top left caption: IAU run, top right caption: Observations TP/ERS period (1992-1997), bottom left caption: INT run, bottom right caption: FREE run.

From these results, an additional remark can be made: as the EKE from the INT run is not very different from the IAU one, it can be concluded that the intermittent assimilation method does not induce major discrepancies when the EKE is of interest, as discussed by Testut (2000).

f. Gulf Stream structure modification

Vertical meridional sections of the horizontal velocity U averaged over a year in the Gulf Stream region is shown in figures 25, 26 and 27, from the surface to a depth of 2000 m for the three types of run. As discussed in Testut et al. (2003), the section from the INT run in figure 26 clearly demonstrates that the data assimilation has consistently modified the three-dimensional structure of the flow when compared to the result from the FREE run in figure 27. For the assimilated run, the zonal velocity is stronger featuring a jet located at a more realistic latitude. If the results from the IAU run in figure 25 is studied, it turns out that the overall flow characteristics are quite similar to the INT run. However a few differences between the INT and IAU run can be noticed. The IAU run seems to have weakened strong gradients such as the one located at latitude 37° N in the INT run. This effect is not so surprising as the IAU filtering method is apparently leading to more balanced ocean states (cf. section 4.a.), and might therefore act as a spatial smoothing filter on the solution. The strong jet velocities seem to reach deeper layers for the IAU run than for than INT run. This might also be explained by an intrinsic difference between the two systems: in the case of the INT run the correction brought from the analyzed state is cut at a depth of 1000 m, leaving the solution unmodified after this level, but in the case of the IAU run, increments are applied to any layer from surface to sea bed.

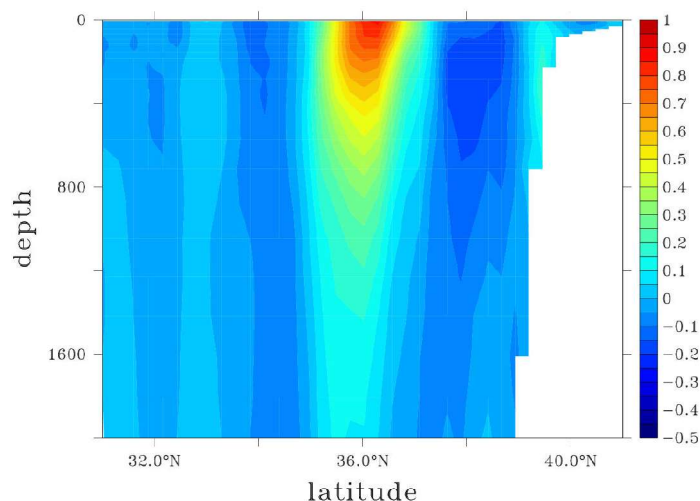


Figure 25: Meridional section in the Gulf Stream region (at 72° W) for the horizontal velocity U (m/s) averaged over a year (04/12/93 to 05/12/93), obtained with the IAU run.

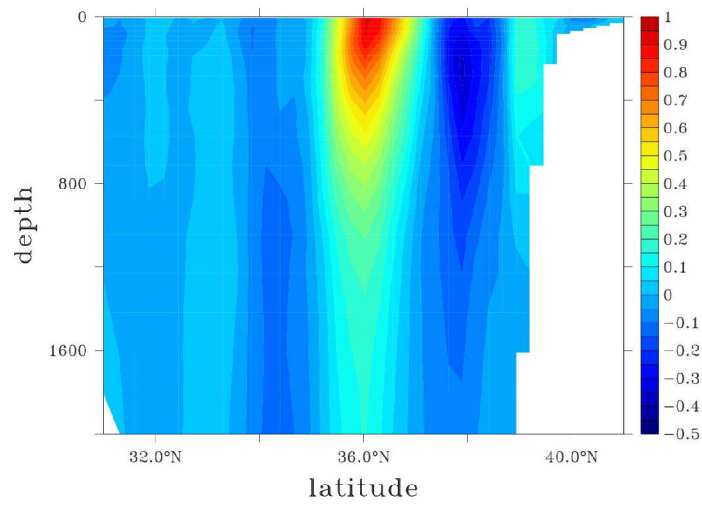


Figure 26: Meridional section in the Gulf Stream region (at 72° W) for the horizontal velocity U (m/s) averaged over a year (04/12/93 to 05/12/93), obtained with the INT run.

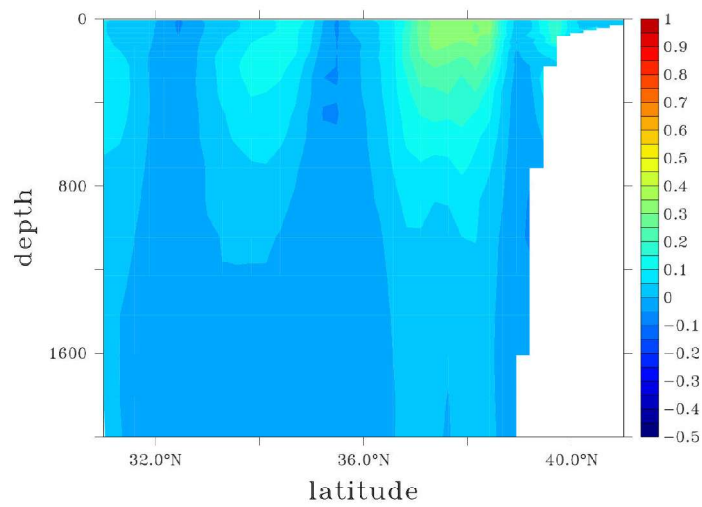


Figure 27: Meridional section in the Gulf Stream region (at 72° W) for the horizontal velocity U (m/s) averaged over a year (04/12/93 to 05/12/93), obtained with the FREE run.

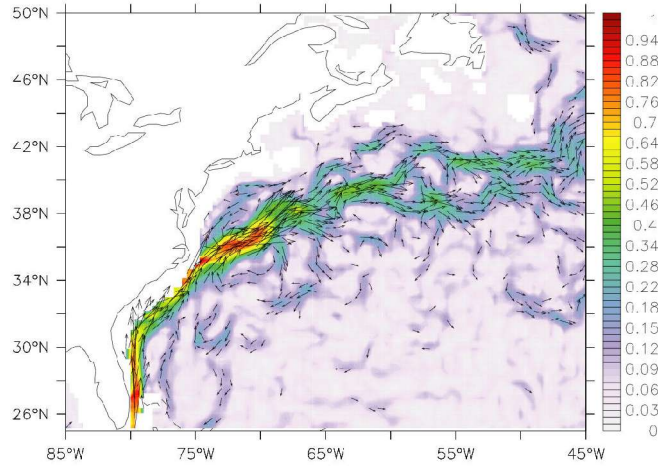


Figure 28: Horizontal velocity (m/s) in the Gulf Stream region at 55 m averaged over a year (04/12/92 to 05/12/93); IAU run.

The horizontal averaged velocity over a year (04/12/92 to 05/12/93) at a depth of 55 m is shown in figures 28, 29 and 30, for the Gulf Stream region. As mentioned by Testut et al.(2003), data assimilation efficiently improves the structure of the Gulf Stream (Fig. 29) when compared to the FREE run (Fig. 30). If the results from the IAU run (Fig. 28) and the INT (Fig. 29) are compared, the overall structure is quite similar, proving that the IAU method also behaves as a consistent data assimilation system.

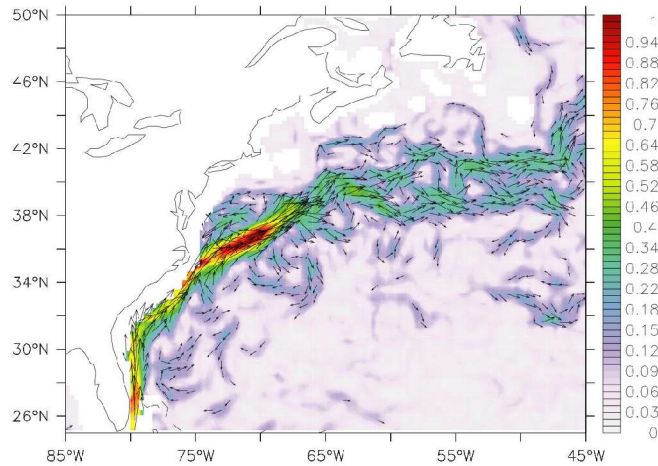


Figure 29: Horizontal velocity (m/s) in the Gulf Stream region at 55 m averaged over a year (04/12/92 to 05/12/93); INT run.

However, it seems that the overall velocities are weaker for the IAU run, which is in good agreement with the remarks done on the vertical sections (Fig. 25, 26 and 27). Again from these results, it appears that the IAU technique also acts as a gradient smoother.

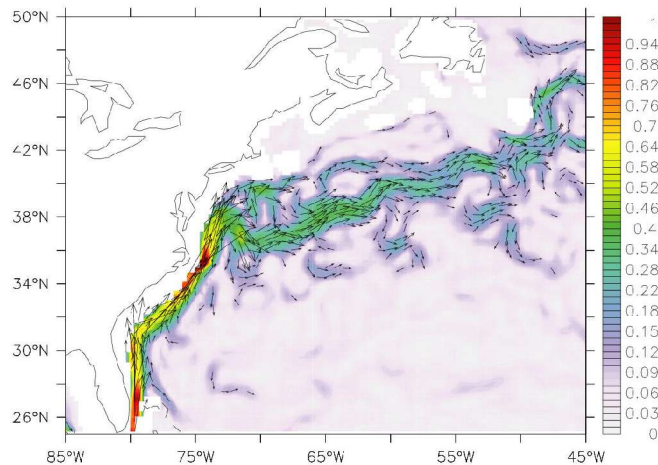


Figure 30: Horizontal velocity (m/s) in the Gulf Stream region at 55 m averaged over a year (04/12/92 to 05/12/93); FREE run.

g. Comparisons with independent data: moorings

In terms of performance, the SST solutions at single grid points have been usually compared to the Levitus (1998) climatology (cf. Fig 12 and 17). A more accurate test can be performed by comparing these results to high frequency recording moorings data. Some grid points selected for high frequency monitoring have also been chosen to correspond to mooring locations (cf. Table 1, section 3.). These moorings were deployed during the WOCE ACM25/26 campaigns in 1993. Unfortunately, these moorings did not provide data for the entire period considered in this study, but comparisons were still possible for a few months, mainly for the temperature. The acquisition period of the instruments was 15 minutes. The original signal being very noisy, the mooring data used in the present study have been filtered by moving average with a filtering window of 12 hours. Figures 31 and 32 are the results of such a comparison for the grid points 2 and 3 located in the Azores current zone and in the Portugal current zone respectively (cf. Fig. 4). For grid point 2 (Fig. 31), the IAU run trajectory is consistent with the overall mooring data trajectory despite being far from similar, and remains obviously closer to the assimilated data. For grid point 3 (Fig. 32), the IAU trajectory is quite different from the mooring data set, however it seems in this case that the assimilated data are very different from the mooring data. Hence, no close agreement can be expected. It can be noted that for these two comparisons, the assimilated data were systematically underestimated when compared to the mooring data sets. This difference might come from the fact that the SST assimilated is the nocturnal SST, while the mooring data set is continuous, as data are recorded all day long.

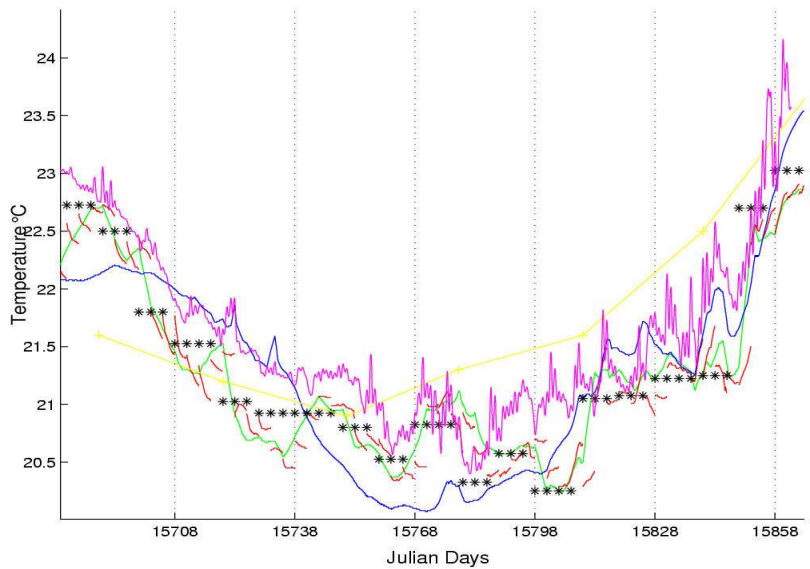


Figure 31: SST at grid point 2; - Free run; - INT run; - IAU run; * Assimilated data; -+- Levitus climatology (1998); - independent data: WOCE moorings. X-axis is the time in Julian days; period from 04/12/92 (15678) to 06/06/93 (15862).

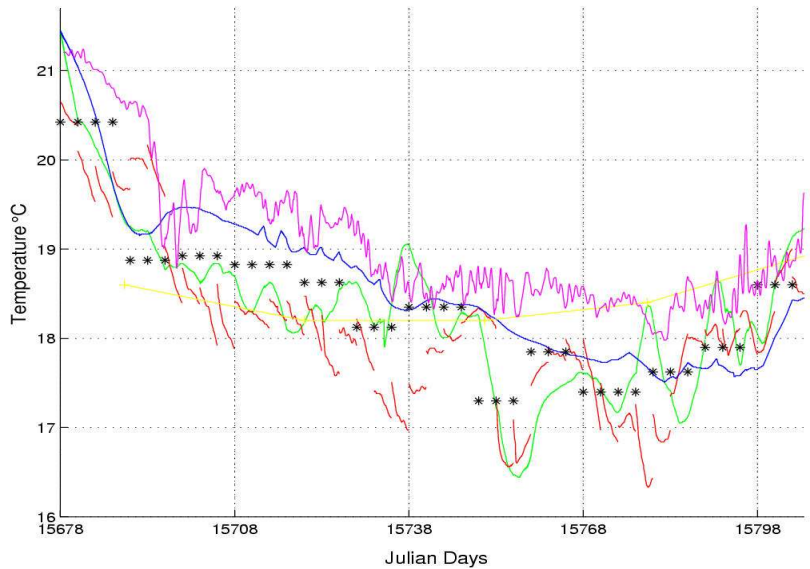


Figure 32: SST at grid point 3; - Free run; - INT run; - IAU run; * Assimilated data; -+- Levitus climatology (1998); - independent data: WOCE moorings. X-axis is the time in Julian days; period from 04/12/92 (15678) to 11/04/93 (15806).

However, any conclusion from this type of comparison has to be cautiously done and remains qualitative as the behavior of the solution at one grid point cannot be directly extrapolated to a larger ocean zone.

5. Conclusion and perspectives

Generally speaking, this study demonstrated that the IAU technique has a lot to offer to operational systems in oceanography.

A review on past and present work on the subject for AGCM and OGCM showed that the algorithm itself is not unique, but that two key ideas on the IAU impact could be picked up, whatever the method: first the IAU method efficiently suppresses spurious oscillations often existing in intermittent data assimilation systems, second it acts like a continuous assimilation method.

The choice, implementation and tests on a specific IAU methodology led to several results and discussions:

- The IAU technique takes out efficiently the high frequency and large amplitude oscillations possibly existing in the case of the intermittent data assimilation system used. Additional tests starting from an ocean state obtained after several months of IAU integration showed that the ocean state was more stabilized than a similar experiment started from an ocean state obtained after several months of intermittent data assimilation. For these specific experiments, no oscillations was seen in the case of an IAU restarted state when oscillations could last for a month in the case of an intermittent restarted state.
- The continuity of the solution is inherent to the IAU method.
- Variables not controlled by the increments such as the horizontal velocities behave in a satisfying manner.
- The overall solution does not seem to be inadequately modified compared to a solution with or without intermittent data assimilation. The possible damping of low frequency waves cited by Polavarapu et al. (2004) has not been noticed in the present study.
- Flow structures enhanced by intermittent data assimilation remain of equivalent improvement in the IAU configuration.
- No particular diagnostic quantity such as the Eddy Kinetic Energy turned out to be invalid for the IAU run results.
- A general behavior is that the IAU tends to weaken strong gradients, which might be explained by the stabilizing effect of the incremental approach: the IAU also seems to act like a spatial smoothing filter.
- With regard to IAU performance in terms of RMS and comparison with independent data, it appears that any improvement in the data assimilation method will also benefit the efficiency on an IAU implemented system.
- The increase in computing time for an IAU implemented OGCM is inevitable due to the very nature of this methodology.

Finally, concerning the choice of such an algorithm for the IAU implementation, the fact that each IAU forecast with incremental forcing stops again at the analyzed time is not a problem in operational forecast, as each free model forecast following this stage, can be considered as the proper forecast. For instance, figure 18 (section 4.c.) shows that the RMS difference between the forecast and the assimilated data for the SST in IAU mode is acceptable compared to the equivalent with intermittent data assimilation. The next step that has to be achieved for the enhancement of the IAU performance is to either impose a systematic incremental correction (no more free model forecast) or to implement a algorithm closely similar to Bloom et al (1996)

including a forecast with incremental corrections twice as long as the forecast done to reach the analyzed state (cf. Fig. 1). Both developments have not been tested in the present study. Furthermore, in the case of a systematic incremental forcing, different versions could be tested. The increment deduced at time i could be applied for a forced forecast from time i to $i+1$. Another possibility could be to apply a variable increment calculated at time i , with stronger weights at the beginning of the assimilation cycle from time $i-1$ to i then with weakening weights from time i to $i+1$. As a result, it seems clear that the main advantages brought up by the IAU technique can be easily enhanced depending on the chosen targets of the forecasting system used.

References

- Alves, O., Balmaseda, M. A., Anderson, D. and Stockdale, T. , 2004: Sensitivity of dynamical seasonal forecasts to ocean initial conditions. *Quart. J. Roy. Meteor. Soc.*, **130**, 647-667, Part B.
- Bloom, S. C., Takacs, L. L., DaSilva, A. M. and Levina, D., 1996: Data assimilation using incremental analysis updates. *Mon. Wea. Rev.*, **124**(6), 1256-1271.
- Brankart, J. M., Testut, C. E., Brasseur, P. and Verron, J., 2003: Implementation of a multivariate data assimilation scheme for isopycnic coordinate ocean models: Application to a 1993-96 hindcast of the North Atlantic Ocean circulation. *J. Geophys. Res.*, **108**(C3), 3074.
- Brasseur, P., Ballabrera, J. and Verron, J., 1999: Assimilation of altimetric observations in a primitive equation model of the Gulf Stream using a Singular Evolutive Extended Kalman filter. *J. Mar. Syst.*, **22**, 269-294.
- Carton, J. A., Chepurin, G., Cao, X. H. and Giese, B., 2000: A simple ocean data assimilation analysis of the global upper ocean 1950-95. Part I: Methodology. *J. Phys. Oceanogr.*, **30**(2), 294-309.
- Derber, J. and Rosati, A., 1989: A global oceanic data assimilation system. *J. Phys. Oceanogr.*, **19**, 1333-1347.
- DeWeaver, E. and Nigam, S., 1997: Dynamics of zonal-mean flow assimilation and implications for winter circulation anomalies. *J. Atmos. Sci.*, **54**(13), 1758-1775.
- Ducet, N., Le Traon, P. and Reverdin, G., 2000: Global high-resolution mapping of ocean circulation from Topex/Poseidon and ERS-1 and -2. *J. Geophys. Res.*, **105**(C8), 19477-19498.
- Huang, B., Kinter, J. L. and Schopf, P. S., 2002: Ocean data assimilation using intermittent analyses and continuous model error correction. *Adv. Atmos. Sci.*, **19**(6), 965-993.
- Levitus, S., Boyer, T.P., Conkright, M.E., O'Brien, T., Antonov, J., Stephens, C., Stathopoulos, L., Johnson, D. and Gelfeld, R., 1998: NOAA Atlas NESDIS 18, WORLD OCEAN DATABASE 1998: Vol. 1: Introduction, *U.S. Gov. Printing Office*, Wash., D.C., 346 pp.

Madec, G., Delecluse, P., Imbard, M. and Levy, C., 1998: OPA8.1, ocean general circulation model reference manual, Notes du pole de modélisation IPSL, **11**.

Pham, D. T., Verron, J. and Roubaud, M. C., 1998: A singular evolutive extended Kalman filter for data assimilation in oceanography. *J. Mar. Syst.*, **16**, 323-340.

Pacanowski, R. C., Dixon, K. and Rosati, A., 1993: The GFDL Modular Ocean Model user guide. Version 1.0. *GFDL Ocean Group Tech. Rep.*, **2**.

Polavarapu, S., Ren, S. H., Clayton, A. M., Sankey, D. and Rochon, Y., 2004: On the relationship between incremental analysis updating and incremental digital filtering. *Mon. Wea. Rev.*, **132**(10), 2495-2502.

Rosati, A., Gudgel, R. and Miyakoda, K., 1995: Decadal analysis produced from an ocean data assimilation system. *Mon. Wea. Rev.*, **123**(7), 2206-2228.

Schubert, S. D., Rood, R. B. and Pfaendtner, J., 1993: An assimilated dataset for earth science applications. *Bull. Amer. Meteor. Soc.*, **74**(12), 2331-2342.

Testut, C. E., 2000: Assimilation de données satellitales avec un filtre de Kalman de rang réduit dans un modèle aux équations primitives de l'océan Atlantique. *PhD thesis*, Université J. Fourier, Grenoble, France.

Testut, C. E., Brasseur, P., Brankart, J. M. and Verron, J., 2003: Assimilation of sea-surface temperature and altimetric observations during 1992-1993 into an eddy permitting primitive equation model of the North Atlantic Ocean. *J. Mar. Syst.*, **40-41**, 291-316.

Weaver, A. T., Vialard, J. and Anderson, D. L. T., 2003: Three- and four-dimensional variational assimilation with a general circulation model of the tropical pacific ocean. Part I: formulation, internal diagnostics and consistency checks. *Mon. Wea. Rev.*, **131** (7), 1360-1378.

Zhu, Y., Guo, R., Cohn, J., Navon, I. M. and Yang, Y., 2003: The geos-3 retrospective data assimilation system: the 6-hour lag case. *Mon. Wea. Rev.*, **131**(9), 2129-2150.

Technical Appendix

A. IAU implementation

1. Model modifications

A few modifications in the source code of OPA 8.1 have been made for the IAU implementation. The following sections indicate the major changes necessary to implement the IAU technique, but an accurate description of the changes is not the purpose of this work for two reasons: first, the modifications needed do not present any severe difficulty for an accustomed OPA user, the IAU algorithm being well documented, therefore, the modifications done here are just a way among several others to code it. Second, as the versions of the code is not unique, it seems more important to understand the IAU methodology itself, exposed in the main document, in order to implement it into a chosen code version.

a. Parlec.F

The parameter *niau* is defined, if *niau=0*, the run will not use the IAU correction (free run), if *niau=1*, the run will call Traiau.F for the IAU incremental forcing.

```
SUBROUTINE parlec
...
  NAMELIST/namiau/ niau
  niau = 0
C
  REWIND( numnam )
  READ ( numnam, namiau )
C
...
```

b.Common.h

In the section II. DYNAMICS AND TRACERS, *dtiau* and *dsiau* three-dimensional arrays are declared. They will contain the IAU increment respectively for T and S at any point of the grid.

```
...
BIGREAL dtiau(jpi,jpj,jpk), dsiau(jpi,jpj,jpk)
...
```

The parameter *niau* has also to be declared, in section V.Diagnostics, as an integer.

```
INTEGER niau
...
COMMON/cimass/....., niau
```

c. Traiau.F

A routine called Traiau.F has been created. Its use is to add the increment to the temperature *ta* and the salinity *sa*. This routine is called by Step.F.

```
SUBROUTINE traiau ( ktask, kt )
...
CC local declarations
```

```

CC =====
      INTEGER ktask, kt, nbpts
#ifdef key_iau
      INTEGER ji, jj, jk
      BIGREAL taiau, saiau, faciau

...
...

C
C =====
C
      faciau = nitend - nit000
      faciau = 1./(faciau*rdt)

      DO 1000 jj = ktask, jpj, ncpu
C
      DO jk = 1, jpk
      DO ji = 1, jpi
C      increment caclulation
          taiau = faciau * dtiau(ji,jj,jk)
          saiau = faciau * dsiau(ji,jj,jk)
C
C
C ...      add it to the general tracer trends
          ta(ji,jj,jk) = ta(ji,jj,jk) + taiau
          sa(ji,jj,jk) = sa(ji,jj,jk) + saiau
          END DO
      END DO
C
C =====
C
      1000 CONTINUE

```

d. Step.F

In the section III Tracer trends, the routine traiau.F is called.

```

SUBROUTINE step ( ktask )

...
C III. Tracer trends
...
  IF ( niau .EQ. 1 ) THEN
      CALL traiau(ktask,istp)

END IF
...

```

e. Dtrlec.F

A section has been added to read the IAU restart file and compute the increment. This modification is placed in such a way that the increment calculation will benefit from the modification post-analysis of the ocean state which occurs in a regular intermittent run to stabilise the analysed state obtained.

```

SUBROUTINE dtrlec
....

IF(niau .EQ. 1) THEN
    WRITE(numout,*) ' '
    WRITE(numout,*) '*** dtrlec read restart and
compute increment'
    WRITE(numout,*) ' '

C   Open file
C
    clname='restartiau'
    open
(numrst,file=clname,status='old',form='unformatted',
    $      access='direct',recl=nrecl8)
C
C   Read tb, sb, tn, sn
C   In this case tb=tf ( t_before = t_forecast )
C   And tn=ta ( t_now = T_analyzed )
C
    READ(numrst,REC=1)
inol,it1,isor1,ipcg1,itkel1,idast1,adatrj
    CALL readn2dglo(numrst,tb ,2*jpk+2,jpk ,readR4)
    CALL readn2dglo(numrst,sb ,3*jpk+2,jpk ,readR4)
    CALL readn2dglo(numrst,tn ,
6*jpk+2+2*jpk+1,jpk,readR4)
    CALL readn2dglo(numrst,sn ,
6*jpk+2+3*jpk+1,jpk,readR4)
    close(numrst)
C
C   stabilize xa
C
    ta(:, :, :) = tn(:, :, :)
    sa(:, :, :) = sn(:, :, :)
    DO itask = 1, ncpu
        CALL tranpc (itask,nit000)
    END DO
C   borne Ta et Sa
    smaxi=FBIGREAL(40.0)
    tmaxi=FBIGREAL(32.0)
    smini=FBIGREAL(23.0)
    DO jj=1,jpj
    DO ji=1,jpi
        DO jk=1,jpk
            sn(ji,jj,jk)=MIN(sn(ji,jj,jk),smaxi)
            sn(ji,jj,jk)=MAX(sn(ji,jj,jk),smini)
            tn(ji,jj,jk)=MIN(tn(ji,jj,jk),tmaxi)
            tn(ji,jj,jk)=MAX(tn(ji,jj,jk),
    $      fsfzpt(sn(ji,jj,jk),FBIGREAL(0.)))
        END DO
    END DO
    END DO
C
C   compute increment (Xa - Xf)
C
    dtiau(:, :, :) = tn(:, :, :) - tb(:, :, :)
    dsiau(:, :, :) = sn(:, :, :) - sb(:, :, :)

```

```

        dtiau(:,:,:) = dtiau(:,:,:) * tmask(:,:,:)
        dsiau(:,:,:) = dsiau(:,:,:) * tmask(:,:,:)
C
C Dump of Xs
        nstepo=0
        print *, 'CALL diawri(1,-1) for Xs dump'
C reset
        tn(:,:,:)=0.e0
        sn(:,:,:)=0.e0
        tb(:,:,:)=0.e0
        sb(:,:,:)=0.e0
        rhopn(:,:,:)=0.e0
ENDIF

```

2. Assimilation system modifications

For similar reasons explained in section A.1., no detailed part of assimilation scripts will be given. It is however important to note few important modifications.

A parameter *doiau* has been introduced, being consequently equal to *True* for an IAU run and *False* for a free run or an run with classic intermittent data assimilation.

The variable *niau* has to change value from 0 to 1, in the same IAU cycle, as *niau* = 0 for the free run preceding the analysis stage, and *niau* = 1 for the run with the IAU increment applied to the model.

B. High frequency outputs

The high frequency outputs were done at any time step, that is every 40 minutes in the present configuration. The grid location of the points are shown in table 2.

<i>Point number</i>	<i>Approx. Latitude N</i>	<i>Approx. Longitude W</i>	<i>X index</i>	<i>Y index</i>	<i>Mooring available</i>
1	18	34	194	117	Yes
2	26	29	209	141	Yes
3	33	22	230	167	Yes
4	26	79	82	144	Yes
5	35.5	66.3	97	176	No
6	60	30	206	288	No

Table 2: High-frequency grid points characteristics.

As a reminder, the index of the grid points are only valid for the NATL3 configuration.